

SANDWICH-STRUCTURE WAVEGUIDES FOR VERY HIGH-POWER GENERATION AND TRANSMISSION USING LEFT-HANDED MATERIALS

Z. Li and T. J. Cui

Center for Computational Electromagnetics and the State Key
Laboratory of Millimeter Waves
Department of Radio Engineering
Southeast University
Nanjing 210096, China

Abstract—The high power generation and transmission for TM modes in a parallel-plate waveguide filled with three-layered medium called sandwich structure are investigated. The transmission power could never exceed the input power of the source in a conventional parallel-plate waveguide filled with homogeneous or inhomogeneous right-handed material (RHM) or homogenous left-handed material (LHM). Based on the stratified medium theory, extremely high power can be generated and transmitted if the waveguide is composed of RHM-LHM-RHM or LHM-RHM-LHM sandwich structure with the medium parameters and layer thickness being properly chosen. Different from the TE case, the dominant mode exists in such a structure is TM_0 mode which can be always supported despite the size of the waveguide. From our numerical results, we find that the high power generation and transmission can be easily realized even in the more realistic case where the LHM is described by the Lorentz medium model.

1. INTRODUCTION

In the past a few years many scientists and engineers have been working on a novel material called left-handed material (LHM) or metamaterial due to its unusual electromagnetic features [2–12, 14, 15, 18, 19]. This kind of material was first theoretically studied by Veselago in 1968 [1]. He pointed out that the permittivity ϵ and permeability μ are simultaneously negative in such a medium. Later in the year of 2000,

Pendry proposed an interesting theory [8] of subwavelength imaging, which has been a hot research topic since then [9, 10, 12, 20].

Recently, in the realization of microwave and optical devices using LHM, new structures including waveguides containing LHM have been in deep concern, which may have prominent applications in the future [11, 12, 14, 15]. It is interesting to note that a super waveguide has been realized by pairing a conventional RHM slab with an equal-thickness LHM slab in a planar waveguide [15]. As reported in [14], if the RHM is air and the LHM is anti-air with permittivity $-\epsilon_0$ and permeability $-\mu_0$, continuously infinite TE modes could be supported in the waveguide and infinite power density could be generated and transmitted under the excitation of a line source. This is obviously unphysical because the ideal $-\epsilon_0$ and $-\mu_0$ can not be realized. When a small retardation δ exists in the LHM, the continuous guided modes reduce to a few discrete TE modes and extremely high power densities could be generated and transmitted along the waveguide [15].

In this work, the concept and physical features of the super waveguide have been inherited and extended to a new sandwich structure waveguide, which is filled with three-layered medium. Since the lowest mode that can be transmitted in a parallel-plate waveguide is TM_0 mode, a new excitation model to generate TM modes is considered. Furthermore, the LHM slab can not exactly reside on the wall of the two-layered waveguide [15], hence it is worth considering whether the high power transmission can still be realized in the sandwich structures. In the next section, exact analysis for this problem are performed based on the stratified medium theory and analytic formulations for the guidance condition of the considered structures are derived in Section 3. Finally, simulation results are given in Section 4, from which we find that the high power generation and transmission can still be realized by the sandwich structure even in a more realistic case where the LHM is treated as a dispersive medium.

2. GENERAL THEORY AND MODEL

In order to explicate the theory universally, a general problem is studied as illustrated in Fig. 1, where a parallel-plate waveguide filled with multi-layered medium is considered. The permittivity and permeability in each layer $R_i (i = 1, 2, \dots, n)$ are denoted by ϵ_i and permeability μ_i respectively. In order only to excite TM modes, an infinite long line source parallel to the y -axis and polarized in the z -direction is placed in region n . The stratified medium and perfect electric conducting (PEC) plates are all assumed to be infinite along the y -direction, which leads to a two dimensional problem. The source

is in the form of $\bar{I} = \hat{z}Il\delta(x - x')\delta(z - z')$ and the two conducting plates (two side walls of the waveguide) are located in the x - y plane. In Fig. 1, the subscript of each symbol indicates the located region of the quantity. For instance, \bar{E}_1 and \bar{H}_1 denote the total electric and magnetic fields in Region 1.

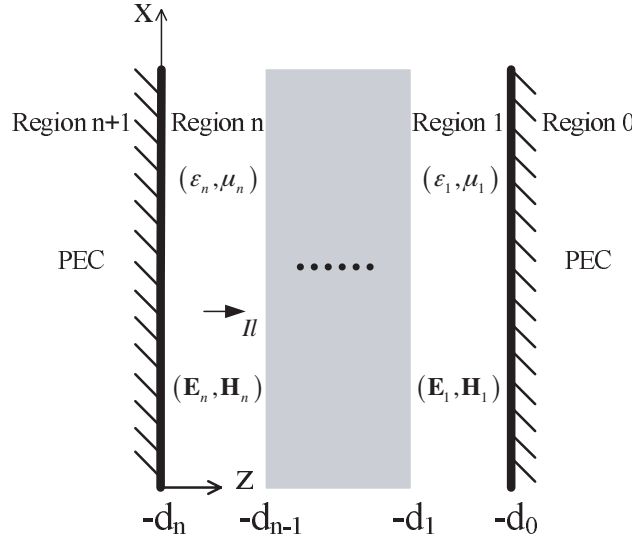


Figure 1. General case for parallel-plate waveguide filled with multi-layered media.

A Cartesian coordinate is set up, in which the two side walls of the waveguide are located at $z = -d_0$ and $z = -d_n$, as illustrated in Fig. 1. Applying the 2D-Wyle identity and the multi-layered media theory [17], the total magnetic field in Region m can be expressed explicitly as

$$H_y^m = \frac{I}{4\pi} \left[\delta(m - n) i\pi k_m H_1^{(1)}(k_m |\bar{\rho} - \bar{\rho}'|) \frac{x - x'}{|\bar{\rho} - \bar{\rho}'|} + 2i \int_0^{+\infty} \frac{k_x}{k_{nz}} \sin[k_x(x - x')] F_m(z, z') dk_x \right], \quad (1)$$

where only the y component of the magnetic field exists. The electric fields can be obtained by $E_x^m = (1/i\omega\epsilon_m)\partial H_y^m/\partial z$ and $E_z^m = (i/\omega\epsilon_m)\partial H_y^m/\partial x$. In Eq. (1), $H_1^{(1)}(\xi)$ is the first-ordered Hankel function and $\delta(m - n)$ is the Kronecker delta function which equals 1 when $m = n$ and equals 0 when $m \neq n$. And $F_m(z, z')$ is a function

which has different forms for different relations of m and n . When $m = n$, the function $F_m(z, z')$ can be written as

$$\begin{aligned}
F_m(z, z') = & [e^{-ik_{mz}(z+z'+2d_{m-1})} \tilde{R}_{m(m-1)} \\
& + e^{-ik_{mz}(z-z'+2d_{m-1}-2d_m)} \tilde{R}_{m(m+1)} \tilde{R}_{m(m-1)} \\
& + e^{ik_{mz}(z+z'+2d_m)} \tilde{R}_{m(m+1)} \\
& + e^{ik_{mz}(z-z'+2d_m-2d_{m-1})} \tilde{R}_{m(m+1)} \tilde{R}_{m(m-1)}] \tilde{M}_m \quad (2)
\end{aligned}$$

When $m \neq n$, Eq. (2) should be replaced by the correct form which can be easily derived according to the multi-layered media theory [17]. In Eq. (2), $\tilde{R}_{i(i-1)}$ is the generalized reflection coefficient

$$\tilde{R}_{i(i-1)} = \frac{R_{i(i-1)} + \tilde{R}_{(i-1)(i-2)} e^{2ik_{i-1z}(d_{i-1}-d_{i-2})}}{1 + R_{i(i-1)} \tilde{R}_{(i-1)(i-2)} e^{2ik_{i-1z}(d_{i-1}-d_{i-2})}} \quad (3)$$

in which

$$R_{i(i-1)} = \frac{\epsilon_{i-1} k_{iz} - \epsilon_i k_{i-1z}}{\epsilon_{i-1} k_{iz} + \epsilon_i k_{i-1z}} \quad (4)$$

is the Fresnel reflection coefficient for TM waves at the two-layered interface. The generalized reflection coefficients \tilde{R}_{10} and $\tilde{R}_{n(n+1)}$ equal to 1 for TM modes at the two PEC planes which are located at $z = -d_0$ and $z = -d_n$.

\tilde{M}_n is a coefficient used to calculate the fields when the source is placed between $-d_1$ and $-d_{n-1}$, which is defined as:

$$\tilde{M}_n = \frac{1}{1 - \tilde{R}_{n(n+1)} \tilde{R}_{n(n-1)} e^{2ik_{nz}(d_n-d_{n-1})}} \quad (5)$$

In all above equations, $k_{nz} = \pm \sqrt{k_n^2 - k_x^2}$ is a double value function of k_x and the sign should be chosen carefully to obey the physical laws. In other words, the real part of k_{nz} must be positive in RHM and negative in LHM for numerical computations. Once all the generalized reflection coefficients $\tilde{R}_{i(i-1)}$ ($i = 1, 2, \dots, n$) and \tilde{M}_n are determined through the boundary condition, the magnetic fields in all layers shown in Eq. (1) can be computed through an integration over the function $F_m(z, z')$. Furthermore, the electric fields and the time-averaged power densities can also be easily obtained. In order to simplify the problem, we only concentrate on the sandwich-structure waveguides thoroughly in the next section.

3. FORMULATIONS AND ANALYSIS OF SANDWICH STRUCTURES

3.1. Guidance Condition for RHM-LHM-RHM Structure

We first consider a structure shown in Fig. 2, in which there are three regions in the waveguide. Regions 1 and 3 are filled with RHM and Region 2 is filled with LHM. In order to explicate the theory specifically, the two regions outside the waveguide are denoted as Regions 0 and 4, respectively. Such a composition is called a RHM-LHM-RHM structure.

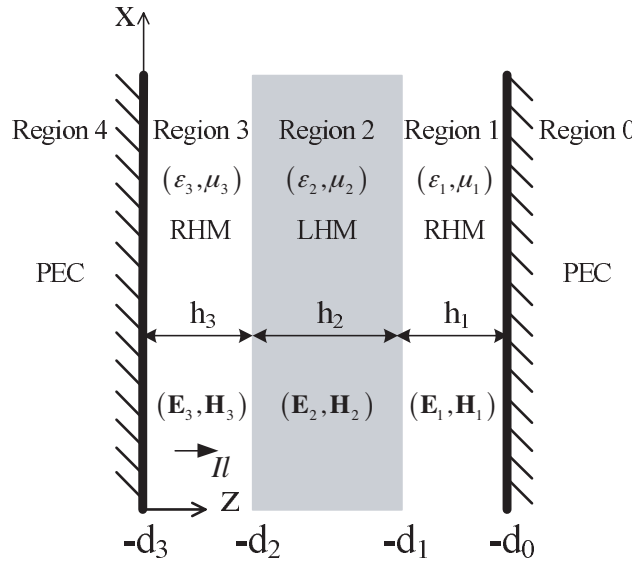


Figure 2. A RHM-LHM-RHM sandwich structure.

In order to deduce the guidance condition in the waveguide, we first give the detailed expressions for \tilde{R}_{21} , \tilde{R}_{32} and \tilde{M}_3 as

$$\tilde{R}_{21} = \frac{R_{21} + \tilde{R}_{10}e^{2ik_{1z}(d_1-d_0)}}{1 + R_{21}\tilde{R}_{10}e^{2ik_{1z}(d_1-d_0)}} \quad (6)$$

$$\tilde{R}_{32} = \frac{R_{32} + \tilde{R}_{21}e^{2ik_{2z}(d_2-d_1)}}{1 + R_{32}\tilde{R}_{21}e^{2ik_{2z}(d_2-d_1)}} \quad (7)$$

$$\tilde{M}_3 = \frac{1}{1 - \tilde{R}_{34}\tilde{R}_{32}e^{2ik_{3z}(d_3-d_2)}} \quad (8)$$

If we denote $T_1 = e^{2ik_{1z}(d_1-d_0)}$, $T_2 = e^{2ik_{2z}(d_2-d_1)}$ and $T_3 = e^{2ik_{3z}(d_3-d_2)}$,

then \widetilde{M}_3 will be simplified as

$$\widetilde{M}_3 = 1 / \left[1 - T_3 \cdot \frac{R_{32} + R_{32}R_{21}T_1 + R_{21}T_2 + T_1T_2}{1 + R_{21}T_1 + R_{32}R_{21}T_2 + R_{32}T_1T_2} \right]. \quad (9)$$

When Regions 1 and 3 are filled with air and Region 2 is an ideal left-handed anti-air with $\mu_2 = -\mu_0$ and $\epsilon_2 = -\epsilon_0$, we have $k_{1z} = -k_{2z} = k_{3z}$ for propagating components of the source with $|k_x| \leq k_0$. Furthermore, $R_{21} = 0$ and $R_{32} = 0$. In such a case, the denominator of \widetilde{M}_3 is simplified as

$$D = 1 - T_1T_2T_3, \quad (10)$$

or

$$D = 1 - e^{2ik_{1z}[2(d_1-d_2)+d_3-d_0]}. \quad (11)$$

We let $h_1 = d_1 - d_0$, $h_2 = d_2 - d_1$, and $h_3 = d_3 - d_2$ represent the thicknesses of the three layers. If $d_3 - d_0 = 2(d_2 - d_1)$ or $h_1 + h_3 = h_2$, i.e., the thickness of Region 2 equals the total thickness of Regions 1 and 3, the denominator becomes zero for all propagating components emitted by the source. In the meantime, the numerator is not equal to zero. Hence each point on the integration path $k_x \in (-k_0, k_0)$ is mapped to a propagating mode.

For the evanescent components of the source ($|k_x| > k_0$), we have $k_{1z} = k_{2z} = k_{3z} = i\sqrt{k_x^2 - k_0^2}$ and $R_{21} \rightarrow \infty, R_{32} \rightarrow \infty$. Then the denominator \widetilde{M}_3 can also be simplified as

$$D = T_2 - T_1T_3, \quad (12)$$

or

$$D = e^{2ik_{2z}[d_2-d_1]} - e^{2ik_{1z}[d_1-d_2+d_3-d_0]}. \quad (13)$$

Again, $D = 0$ in any cases if $d_3 - d_0 = 2(d_2 - d_1)$ or $h_1 + h_3 = h_2$. Thus, all points on the integration path $|k_x| \in (k_0, \infty)$ are also poles of \widetilde{M}_3 . As a consequence, continuously evanescent modes can be guided in the waveguide. The above phenomena are quite similar to those in the two-layered waveguide with the TE excitation [15].

However, the ideal lossless left-handed anti-air has been shown unphysical [9]. In the realistic artificial LHM, a retardation or loss always exists. When a retardation δ exists in LHM in Region 2, the relative permittivity and permeability can be written as $\epsilon_{2r} = -(1 + \delta)$ and $\mu_{2r} = -1/(1 + \delta)$ [14, 15].

For propagating components of the source with $|k_x| \leq k_0$, we have $k_{1z} = -k_{2z} = k_{3z}$, $R_{21} = -\delta/(2 + \delta)$ and $R_{32} = \delta/(2 + \delta)$. Under this condition, the infinite guided modes reduce to a few discrete TM modes. If we denote $h_1 = x$ and $h_2 = h$, then h_3 will be $h - x$. That

is, $T_1 = e^{2ik_{1z}x}$, $T_2 = e^{-2ik_{1z}h}$, and $T_3 = e^{2ik_{1z}(h-x)}$. Furthermore, \widetilde{M}_3 could be simplified as

$$\widetilde{M}_3 = \frac{4 + 4\delta + [\delta(2 + \delta)e^{2ik_{1z}x} - \delta^2][e^{-2ik_{1z}h} - 1]}{4i\delta \sin(k_{1z}h)\{\delta \cos(k_{1z}h) - (2 + \delta) \cos(k_{1z}(2x - h))\}} \quad (14)$$

Obviously, the expression for \widetilde{M}_3 is much more complicated than that in Ref. [15]. But we can find that \widetilde{M}_3 is also inversely proportional to δ . As a consequence, a small δ could give rise to tremendous value of the field, making it possible for high-power transmission. From Eq. (14), we could easily obtain the guidance condition for the RHM-LHM-RHM structure waveguide, which corresponds to the poles in the integrand: $\sin(k_{1z}h) = 0$. Hence the guided modes are determined by $k_{1z}h = m\pi$ ($m = 0, 1, 2, \dots$).

For evanescent components of the source with $|k_x| > k_0$, we have $k_{1z} = k_{2z} = k_{3z} = i\alpha$, $R_{21} = -(2 + \delta)/\delta$ and $R_{32} = (2 + \delta)/\delta$. Under this condition, \widetilde{M}_3 could be simplified as

$$\widetilde{M}_3 = \frac{\delta^2 - \delta(2 + \delta)[e^{-2\alpha x} - e^{2\alpha(h-x)}] - (2 + \delta)^2 e^{2\alpha h}}{4(2 + \delta) \operatorname{sh}(\alpha h)\{\delta \operatorname{ch}[\alpha(2x - h)] - (2 + \delta) \operatorname{ch}(\alpha h)\}}. \quad (15)$$

Since the denominator could never be zero in any case, the evanescent components can never be guided.

Generally, if a retardation δ exists in LHM and the condition $h_1 + h_3 = h_2$ is satisfied, there will be a discrete number of guided modes to be propagated in the waveguide, where the guidance condition can be explicitly written as

$$k_x = \pm \sqrt{k^2 - (m\pi/h)^2}, \quad (m = 0, 1, 2, \dots) \quad (16)$$

in which k is the wavenumber in free space and $m\pi/h \leq k$. Here, ‘+’ indicates the guided modes propagating upwards to the source, and ‘-’ indicates the guided modes propagating downwards to the source. We remark that TM_0 mode can always be supported in the parallel-plate waveguide, which is quite different from the TE case [15], where the lowest TE mode is TE_1 that may not be supported if $h < \lambda/2$. The reason that the TM_0 mode has no cut-off unlike the TE mode is due to the PEC boundary condition imposed. Hence, the high-power transmission can always be supported for the TM mode.

Another important fact is that the sandwich structure is more general than the two-layered structure reported in Ref. [15]. Actually, when $h_1 = h_2$ and $h_3 = 0$, the sandwich structure will reduce to the two-layered one [15]. And in realistic applications, it is hard to reside

the LHM slab exactly on the PEC wall of the waveguide in the two-layered structure [15]. In the case when a small gap exists between the LHM slab and the PEC wall, the general sandwich model can be applied in the exact analysis and numerical simulations.

3.2. Guidance Condition for LHM-RHM-LHM Structure

Now we consider a LHM-RHM-LHM structure waveguide shown in Fig. 3, where Regions 1 and 3 are filled with LHM and Region 2 is filled with RHM. Through complicated deductions, one can prove that if the LHM in Regions 1 and 3 are ideal left-handed anti-air and the condition $h_1 + h_3 = h_2$ is satisfied, the similar unphysical phenomena arise to those in the RHM-LHM-RHM waveguide. Hence we only focus our attention on the case when there is a retardation δ existing in LHM.

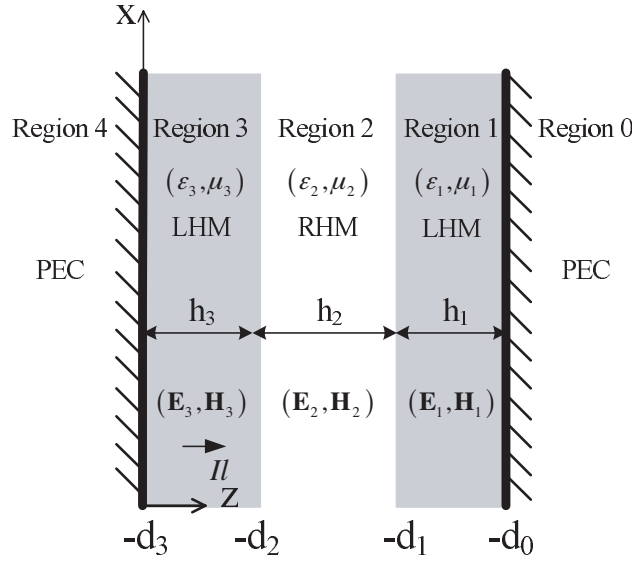


Figure 3. A LHM-RHM-LHM sandwich structure.

For propagating components of the source with $|k_x| \leq k_0$, we have $k_{1z} = -k_{2z} = k_{3z}$, $R_{21} = \delta/(2 + \delta)$ and $R_{32} = -\delta/(2 + \delta)$. Thus, \widetilde{M}_3 can be written as

$$\widetilde{M}_3 = \frac{4 + 4\delta + [\delta(2 + \delta)e^{2ik_{1z}x} + \delta^2][1 - e^{-2ik_{1z}x}]}{4i\delta \sin(k_{1z}h) \{ \delta \cos(k_{1z}h) + (2 + \delta) \cos(k_{1z}(2x - h)) \}}. \quad (17)$$

For evanescent components of the source with ($|k_x| > k_0$), we have

$k_{1z} = k_{2z} = k_{3z} = i\alpha$, $R_{21} = (2 + \delta)/\delta$ and $R_{32} = -(2 + \delta)/\delta$. Under this condition, \widetilde{M}_3 could be simplified as

$$\widetilde{M}_3 = \frac{\delta^2 + \delta(2 + \delta)[e^{-2\alpha x} - e^{2\alpha(h-x)}] - (2 + \delta)^2 e^{2\alpha h}}{4(2 + \delta)sh(\alpha h)\{\delta ch[\alpha(2x - h)] + (2 + \delta)ch(\alpha h)\}}. \quad (18)$$

Clearly, the expressions for \widetilde{M}_3 are very similar to those in the RHM-LHM-RHM structure, where \widetilde{M}_3 are also inversely proportional to δ . From Eqs. (17) and (14), the LHM-RHM-LHM waveguide has the same guidance conditions as that of the RHM-LHM-RHM waveguide.

Comparing the two structures discussed above, we make a conclusion that both of them can be used to fulfill the high-power generation and transmission. The RHM-LHM-RHM configuration and the LHM-RHM-LHM configuration are complementary to each other, which has been proved through a recent theorem [13] by Pendry and Ramakrishna. In this work, the two structures are also complementary pairs that show complementary physical features in power transmission. If a small retardation δ is added to the permittivity and permeability of LHM factitiously, the high-power generation and transmission could be implemented in both structures and will be validated through numerical results in the next section.

3.3. Guidance Condition for a Realistic Structure

As indicated in [4], LHM must be treated as a dispersive media, in which the permittivity and permeability are both functions of frequency. In order to make our discussions more close to practice, Lorentz medium model is used to express the dispersive relation as follows:

$$\epsilon_r(\omega) = 1 - \frac{\omega_{ep}^2 - \omega_{eo}^2}{\omega^2 - \omega_{eo}^2 - i\gamma\omega}, \quad (19)$$

$$\mu_r(\omega) = 1 - \frac{\omega_{mp}^2 - \omega_{mo}^2}{\omega^2 - \omega_{mo}^2 - i\gamma\omega}, \quad (20)$$

where ω_{ep} and ω_{mp} are electric and magnetic resonance frequencies, ω_{eo} and ω_{mo} are electric and magnetic plasma frequencies, and γ is the loss factor. Obviously, ϵ_r and μ_r are determined by several independent variables, which makes derivations of the analytic expressions of the guidance condition of the above two sandwich structures very difficult or even impossible. However, from our numerical simulations, we find that even this realistic model is used to describe the LHM, the generated and transmitted power densities are still much larger than that in the conventional waveguide.

4. SIMULATION RESULTS AND DISCUSSIONS

In this section, we will give the numerical results of the transmission power density in the partially filled parallel-plate waveguides excited by a z -directed line current source. The coordinate of each point is given in the form of (x, z) with the unit of meters. The momentum of the line source is set as $Il = 10^{-3}$ A·m, and the operating frequency is 1 GHz. Considering that in realistic cases LHM is always lossy, we specify the relative permittivity $\epsilon_r = -(1 + \delta) + i\gamma_e$ and permeability $\mu_r = -1/(1 + \delta) + i\gamma_m$ for LHM. The lossy parameters γ_e and γ_m are both set to 10^{-4} in the following computations except when the Lorentz medium model is used.

We first consider a RHM-LHM waveguide, in which $d_0 = -0.12$ m, $d_1 = -0.06$ m, and $d_2 = 0.0$ m. The source is located at $(0.0, 0.06)$. The whole width of the waveguide is 0.12 m, which is smaller than half of the wavelength. Hence higher TM modes are not supported and only the dominant TM₀ mode is excited and transmitted. The real part of the Poynting vector $P_x = \text{Re}(E_z H_y^*)$, which represents the time-averaged power density propagating along the waveguide, will be computed in the following simulations.

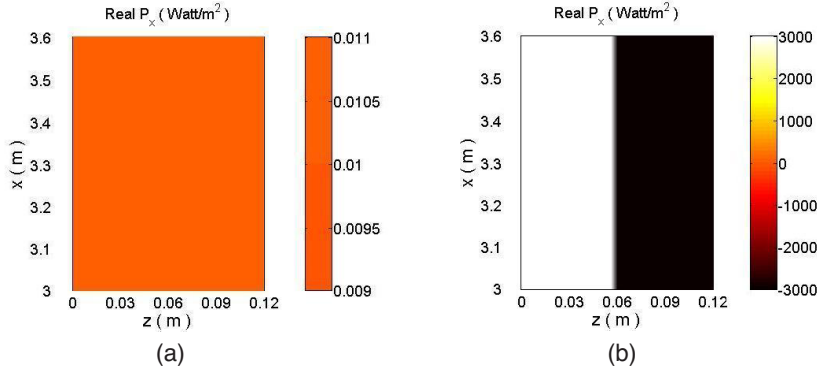


Figure 4. The time-averaged power densities propagating in the waveguide along a section from $x_1 = 3$ m to $x_2 = 3.6$ m. (a) In the air-filled waveguide. (b) In the RHM-LHM waveguide with $\delta = 10^{-4}$.

For comparison, the time-averaged power density propagating in an air-filled waveguide along a section from $x_1 = 3$ m to $x_2 = 3.6$ m is given in Fig. 4(a). For the dominant TM₀ mode, the field values are constants along the z direction, and the value of time-averaged power density is about 10^{-2} W/m². Under the excitation of the same source, the time-average power density propagating in a two-layered super

waveguide [15] along the same section is demonstrated in Fig. 4(b), in which the waveguide is partially filled by LHM with a slight retardation $\delta = 10^{-4}$. In this case, the time-average power density in the air region is as high as $3 \times 10^3 \text{ W/m}^2$, which is nearly 3×10^5 times larger than that in the conventional air-filled waveguide.

We remark that this important phenomenon also obey the physical laws because the total time-average power density flowing in the RHM part towards $+x$ direction is nearly the same as that flowing in the LHM part towards $-x$ direction in Fig. 4(b). Hence the net power through the whole cross section is small. However, extremely high power is generated and transmitted in both RHM and LHM regions.

Now we concentrate on the sandwich structures shown in Figs. 2 and 3. In the RHM-LHM-RHM structure, the boundaries are set as $d_0 = -0.12 \text{ m}$, $d_1 = -0.09 \text{ m}$, $d_2 = -0.03 \text{ m}$, and $d_3 = 0.0 \text{ m}$. Hence the LHM slab is located symmetrically in the waveguide, and the source is placed at $(0.0, 0.015)$. Apparently the condition $h_2 = h_1 + h_3$ is satisfied and only TM_0 mode exists in the waveguide.

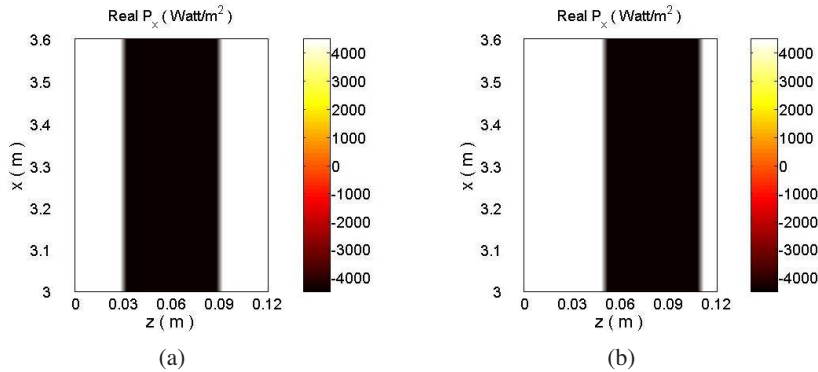


Figure 5. The time-averaged power densities propagating in the RHM-LHM-RHM waveguides with $\delta = 10^{-4}$ along a section from $x_1 = 3 \text{ m}$ to $x_2 = 3.6 \text{ m}$. (a) Symmetrically filled. (b) Unsymmetrically filled.

When $\delta = 0.0001$, the time-averaged power density is drawn in Fig. 5(a), which is nearly $4 \times 10^3 \text{ W/m}^2$ and is much larger than that in the RHM-LHM waveguide. If we keep the source unmoved and change the interfaces of RHM and LHM slabs as $d_0 = -0.12 \text{ m}$, $d_1 = -0.11 \text{ m}$, $d_2 = -0.05 \text{ m}$, and $d_3 = 0.0 \text{ m}$, which means that the LHM slab is located unsymmetrically in the waveguide, the condition $h_2 = h_1 + h_3$ is still satisfied. Under this condition, the time-averaged power density is shown in Fig. 5(b). It is clear that the high-power transmission is

again obtained. It is interesting to note that if we keep the width of the LHM slab unchanged and move it freely in the waveguide, the averaged power density in either RHM or LHM region does not vary at all. Therefore, once the condition $h_2 = h_1 + h_3$ is satisfied, the position at which we place the LHM slab does not affect the field distribution, thus does not affect the averaged power density in all three regions.

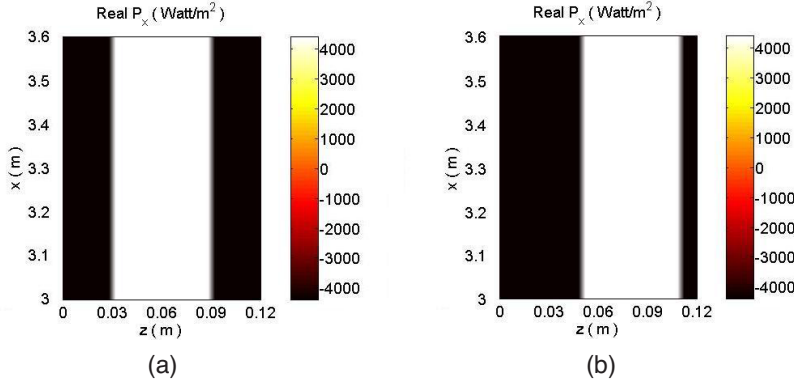


Figure 6. The time-averaged power densities propagating in the LHM-RHM-LHM waveguides with $\delta = 10^{-4}$ along a section from $x_1 = 3$ m to $x_2 = 3.6$ m. (a) Symmetrically filled. (b) Unsymmetrically filled.

Next we turn on to observe the transmitted power densities in the LHM-RHM-LHM structure. All conditions remain unchanged except that the RHM and LHM slabs exchange their positions. The numerical results are shown in Figs. 6(a) and 6(b). We find that the characteristics of the high-power generation and transmission have been maintained. If we observe the differences between Figs. 5 and 6 closely, we could find that the two structures are physically complementary and the numerical results also prove that they are a complementary pair. The RHM-LHM-RHM structure is more practical in construction and could find potential applications in microwave and optical devices.

If we set $d_0 = -0.12$ m, $d_1 = -0.09$ m, $d_2 = -0.05$ m, and $d_3 = 0.0$ m, which means that the condition $h_2 = h_1 + h_3$ is not satisfied, we have computed the time-averaged power density in the same section of the RHM-LHM-RHM structure, as shown in Fig. 7. Apparently the time-averaged power density is much smaller in this case.

Now we move on to watch the cases when the retardation δ is much larger in the LHM. For $\delta = 0.05$, we have computed the time-

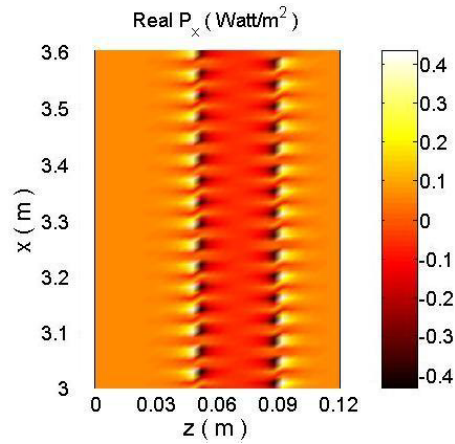


Figure 7. The time-averaged power density propagating in the RHM-LHM-RHM waveguide along a section from $x_1 = 3\text{ m}$ to $x_2 = 3.6\text{ m}$ when the condition $h_2 = h_1 + h_3$ is not satisfied.

averaged power density for both the RHM-LHM-RHM and LHM-RHM-LHM structures in the same section as all the cases above and show them in Fig. 8. We can find that when the retardation δ becomes larger and larger, the time-averaged power density decreases, but is still larger than that in the conventional waveguide filled with purely homogeneous RHM or LHM.

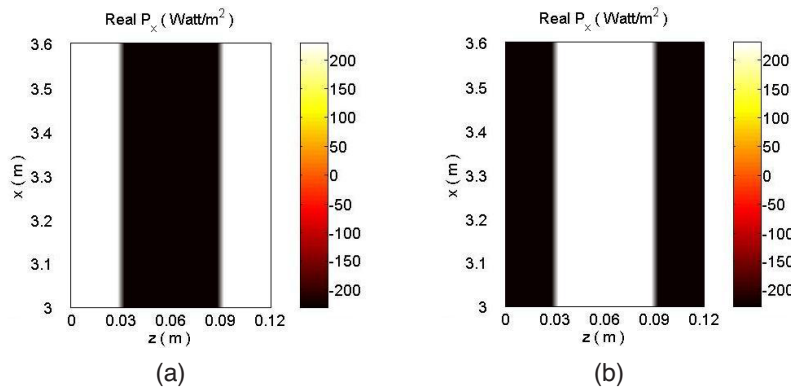


Figure 8. The time-averaged power densities propagating in the sandwich structure waveguides with $\delta = 0.05$ along a section from $x_1 = 3\text{ m}$ to $x_2 = 3.6\text{ m}$. (a) RHM-LHM-RHM structure case. (b) LHM-RHM-LHM structure case.

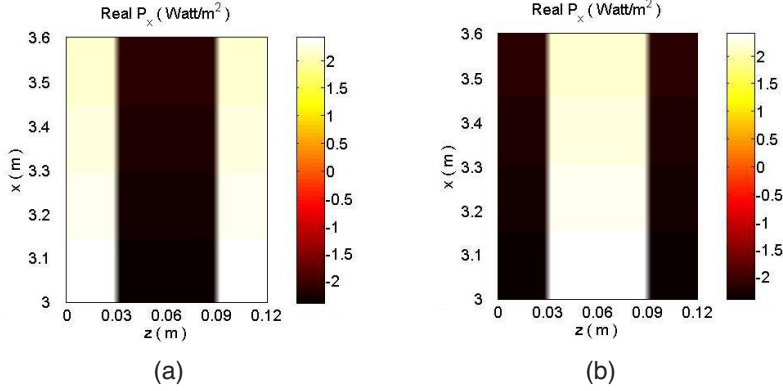


Figure 9. The time-averaged power densities propagating in the sandwich structure waveguides along a section from $x_1 = 3$ m to $x_2 = 3.6$ m. The LHM is expressed by Lorentz medium model using the following parameters: $f_{e0} = 0.12$ GHz, $f_{m0} = 0.14$ GHz, $f_{ep} = 1.39$ GHz, $f_{mp} = 1.43$ GHz, and $\gamma = 3.21$ MHz (a) RHM-LHM-RHM structure case. (b) LHM-RHM-LHM structure case.

Furthermore, we consider a more realistic situation when the LHM is dispersive and highly dissipative, in which the Lorentz medium model is used to describe the relative permittivity and permeability as shown in Eqs. (19) and (20). The parameters are chosen as $f_{e0} = 0.12$ GHz, $f_{m0} = 0.14$ GHz, $f_{ep} = 1.39$ GHz, $f_{mp} = 1.43$ GHz, and the loss factor is chosen as $\gamma = 3.21$ MHz, we obtain $\epsilon_r = -0.9457 + i0.001$ and $\mu_r = -1.0658 + i0.0011$ from the Lorentz medium model at the frequency of 1 GHz. Obviously, a much larger loss exists in this case. For such a realistic RHM-LHM-RHM and a LHM-RHM-LHM structure, we have computed the time-averaged power density, as shown in Fig. 9(a) and Fig. 9(b). From these two figures, we observe that the transmission power in the realistic sandwich-structure waveguide is about 240 times larger than that in the conventional air-filled waveguide, which makes high-power generation and transmission possible in realistic situation.

Finally, we compute the net power through the whole cross section for all the above cases and observe that the net power sustains at a certain level of about 0.01 Watt, which is nearly the same as the input power of the source. So it does not violate the rule of energy conservation.

5. CONCLUSION

In this work, guidance conditions for the TM modes in parallel-plate waveguide filled with different sandwich structures (RHM-LHM-RHM or LHM-RHM-LHM) are developed. From our analysis and numerical results, we find that extremely high power generation and transmission can be obtained when the condition $h_2 = h_1 + h_3$ is satisfied, and performances of this structure are even better than that considered in [15]. Finally, we show that even in the more realistic case where the LHM is described by the Lorentz model, such important properties can still be realized.

ACKNOWLEDGMENT

This work was supported in part by the National Science Foundation of China under Grant Nos. 60671015 and 60496317, in part by the National Basic Research Program (973) of China under Grant No. 2004CB719802, and in part by the National Doctoral Foundation of China under Grant No. 20040286010. Email: tjcui@seu.edu.cn.

REFERENCES

1. Veselago, V. G., "The electrodynamics of substances with simultaneously negative values of ϵ and μ ," *Sov. Phys. Usp.*, Vol. 10, 509, 1968.
2. Pendry, J. B., A. J. Holden, W. J. Stewart, and I. Youngs, "Extremely low frequency plasmons in metallic mesostructures," *Phys. Rev. Lett.*, Vol. 76, 4773, 1996.
3. Pendry, J. B., A. J. Holden, D. J. Robbins, and W. J. Stewart, "Magnetism from conductors and enhanced nonlinear phenomena," *IEEE Trans. Microwave Theory Tech.*, Vol. 47, 2075, 1999.
4. Shelby, R. A., D. R. Smith, and S. Schultz, "Experimental verification of a negative index of refraction," *Science*, Vol. 292, 77, 2001.
5. Smith, D. R., W. J. Padilla, D. C. Vier, S. C. Nemat-Nasser, and S. Schultz, "Composite medium with simultaneously negative permeability and permittivity," *Phys. Rev. Lett.*, Vol. 84, 4184, 2000.
6. Grbic, A. and G. V. Eleftheriades, "Growing evanescent waves in negative-refractive-index transmission-line media," *Appl. Phys. Lett.*, Vol. 82, 1815, 2003.

7. Caloz, C. and T. Itoh, *Electromagnetic Metamaterials: Transmission Line Theory and Microwave Applications*, Wiley, New York, 2004.
8. Pendry, J. B., "Negative refraction makes a perfect lens," *Phys. Rev. Lett.*, Vol. 85, 3966, 2000.
9. Garcia, N. and M. Nieto-Vesperinas, "Left-handed materials do not make a perfect lens," *Phys. Rev. Lett.*, Vol. 88, 207403, 2002.
10. Ramakrishna, S. A. and J. B. Pendry, "The asymmetric lossy near-perfect lens," *J. Modern Opt.*, Vol. 49, 1747, 2002.
11. Engheta, N., "An idea for thin subwavelength cavity resonators using metamaterials with negative permittivity and permeability," *IEEE Antennas Wireless Propagat. Lett.*, Vol. 1, 10, 2002.
12. Nefedov, I. S. and S. A. Tretyakov, "Waveguide containing a backward-wave slab," *Radio Sci.*, Vol. 38, 1101, 2003.
13. Pendry, J. B. and S. A. Ramakrishna, "Focusing light using negative refraction," *J. Phys.: Condens. Matter*, Vol. 15, 6345–6364, 2003.
14. Cui, T. J., Q. Cheng, W. B. Lu, Q. Jiang, and J. A. Kong, "Localization of electromagnetic energy using a left-handed-medium slab," *Phys. Rev. B*, Vol. 71, 045114, 2005.
15. Cheng, Q. and T. J. Cui, "High-power generation and transmission through a left-handed material," *Phys. Rev. B*, Vol. 72, 113112, 2005.
16. Harrington, R. F., *Time-Harmonic Electromagnetic Fields*, McGraw-Hill Book Co., New York, 1961.
17. Chew, W. C., *Wave and Fields in Inhomogeneous Media*, 2nd edition, IEEE Press, New York, 1995.
18. Xu, W., L. W. Li, H. Y. Yao, T. S. Yeo, and Q. Wu, "Left-handed material effects on waves modes and resonant frequencies: filled waveguide structures and substrate-loaded patch antennas," *Journal of Electromagnetic Waves and Applications*, Vol. 19, No. 15, 2033–2047, 2005.
19. Chew, W. C., "Some reflections on double negative materials," *Progress In Electromagnetics Research*, PIER 51, 1–26, 2005.
20. Wongkasem, N., A. Akyurtlu, J. Li, A. Tibolt, Z. Kang, and W. D. Goodhue, "Novel broadband terahertz negative refractive index metamaterials: analysis and experiment," *Progress In Electromagnetics Research*, PIER 64, 205–218, 2006.